Article

Palladium-Catalyzed Highly Regioselective Hydrocarboxylation of Alkynes with Carbon Dioxide

Wenfang Xiong, Fuxing Shi, Ruixiang Cheng, Baiyao Zhu, Lu Wang, Pengquan Chen, Hongming Lou, Wanqing Wu, Chaorong Qi, Ming Lei, and Huanfeng Jiang

ACS Catal., **Just Accepted Manuscript** • DOI: 10.1021/acscatal.0c01687 • Publication Date (Web): 25 Jun 2020

Palladium-Catalyzed Highly Regioselective Hydrocarboxylation of Alkynes with Carbon Dioxide

Wenfang Xiong,[+†] Fuxing Shi,[+‡] Ruixiang Cheng,[†] Baiyao Zhu,[†] Lu Wang,[†] Pengquan Chen,[†] Hongming Lou,[†] Wanqing Wu,[†] Chaorong Qi,*[†] Ming Lei*[‡] and Huanfeng Jiang*[†]

[†]Key Laboratory of Functional Molecular Engineering of Guangdong Province, School of Chemistry and Chemical Engineering, South China University of Technology, Guangzhou 510640, China.

[‡] State Key Laboratory of Chemical Resource Engineering, Institute of Computational Chemistry, College of Chemistry, Beijing University of Chemical Technology, Beijing 100029, China

[+] These authors contributed equally to this work

Supporting Information

ABSTRACT: A Pd-catalyzed highly regioselective hydrocarboxylation of alkynes with carbon dioxide has been established. By the combination of $Pd(PPh_3)_4$ and 2,2'-Bis(diphenylphosphino)-1,1'-binaphthalene (Binap), a variety of functionalized alkynes, including aryl alkynes, aliphatic alkynes, propargylamines and propargyl ethers, could be leveraged to provide a wide array of α-acrylic acids in high yields with high regioselectivity under mild reaction conditions. Experimental and DFT mechanistic studies revealed that this reaction proceeded *via* the cyclopalladation process of alkynes and carbon dioxide in the presence of Binap to generate a five-membered palladalactones intermediate, and enabled the formation of the Markovnikov adducts. Moreover, this strategy provided an effective method for the late-stage functionalization of alkyne-containing complicated molecules, including natural products and pharmaceuticals.

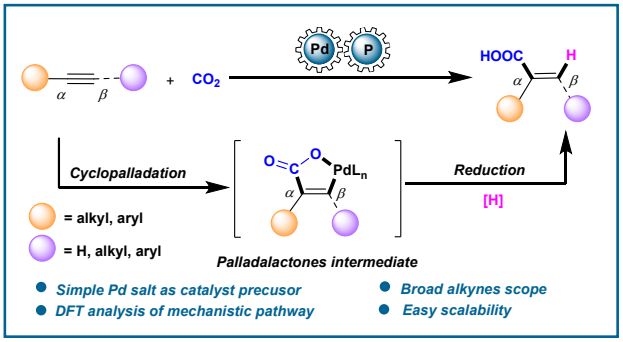

KEYWORDS: alkynes, carbon dioxide, DFT calculation, hydrocarboxylation, Markovnikov addition, palladium

INTRODUCTION

Alkynes functionalization is one of the most dynamic and synthetically powerful research areas in modern synthetic chemistry because it enables the directly synthesis of functionalized alkenes.[1] The control of regioselectivity and stereoselectivity, however, remains a formidable challenge in developing such transformations, which inspires a series of catalytic systems to address these selectivity issues, especially for the hydrofunctionalization of alkynes.[2]

Transition metal-catalyzed carboxylation reactions with CO_2 have emerged as a powerful and versatile strategy for the direct synthesis of carboxylic acids,[3] which represent an important class of molecules, widely existed in natural products[4] and pharmaceuticals[5] (Scheme 1A). Among them, the hydrocarboxylation of alkynes with CO_2 is one of the most straightforward and atom-economical methodology. In the early years, noncatalytic approaches using a stoichiometric amount of Ni reagents were relied to implement the hydrocarboxylation of alkynes and CO_2.[6] Recently, by the use of reductants, such as $ZnEt_2$, silane and Mn, a series of transition-metal catalytic systems for the hydrocarboxylation of alkynes with CO_2 have been successfully developed. For instance, Ma,[7a] Tsuji,[7b] Martin,[7c, 7f] et al. reported Ni- or Cu-catalyzed hydrocarboxylation of internal alkynes with CO_2 in recent years.[7] These catalytic transformations usually proceeded through Ni-catalyzed cyclometallation or Cu-catalyzed hydrometallization process, and some challenging issues still remain in terms of substrate scope and catalyst efficiency. Thus, the development of new catalytic systems to address these issues is of great significant but extremely challenging.

Palladium-catalyzed carbon-carbon bond and carbon-heteroatom bond formation reactions have been extensively investigated over the past several decades, owing to the inherent advantages of versatility, high reactivity and high selectivity of palladium reagents.[8] However, only a few noteworthy research works focused on the Pd-catalyzed direct carboxylation reactions involving CO_2 and their mechanisms.[9] So far, there are two representative strategies,[10] including i) the carboxylation of aryl halide and benzyl halide through the insertion of CO_2 to C-Pd bond (Scheme 1B, a) [10b,10d,10h]; and ii) the carboxylation of σ-allylpalladium species through the nucleophilic addition,

which derived from the hydropalladation process of allenes and dienes or the

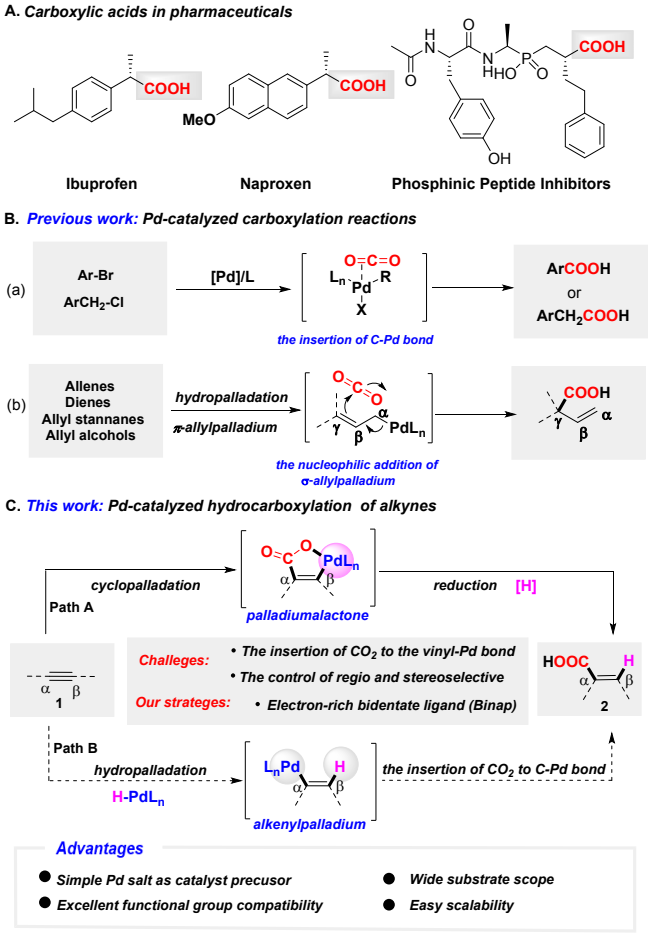

Scheme 1. Palladium-catalyzed hydrocarboxylation of alkynes with CO_2 and their applications in organic synthesis.

allylpalladium process of allyl stannanes and allylic alcohols (Scheme 1B, b).[10a,10c,10e,10f,10g,10i] Surprisingly, while these systems allow for the carboxylation of specific substrate classes, the Pd-catalyzed direct hydrocarboxylation of readily available alkynes with CO_2 has remained almost unexplored to date. One challenge associated with this transformation may be the insertion of CO_2 to vinyl-Pd bond of alkenylpalladium intermediate,[9b,10d] which was regarded as a typical intermediate in the hydrofunctionalization of alkynes.[2] The underlying reason may be due to the C-Pd bonds of organopalladium intermediates are relatively nonpolar, and display rather low reactivity toward those polar electrophiles.[9b, 11] So CO_2 as an electrophile is difficult to react with organopalladium intermediates in most cases. Another challenge in developing Pd-catalyzed direct hydrocarboxylation of alkynes with CO_2 is to control chemo-, regio- and stereoselectivity, because this reaction can potentially produce overreduction byproduct and various isomers of products. Based on our recent works about Pd-catalyzed coupling reactions of unsaturated hydrocarbons,[12] we envisioned that a sufficient electron-rich bidentate phosphine ligand might enhance the catalyst activity of Pd catalyst and then promote the hydrocarboxylation of alkynes and CO_2 in the presence of an appropriate reducing agent. Herein, we reported the success of this approach by the use of new catalytic system consisting of simple palladium catalyst and bidentate phosphine ligand, enabling the synthesis of various α-acrylic acids in a highly regio- and stereoselective manner (Scheme 1C). Moreover, density functional theory calculations (DFT) demonstrated this protocol proceeded the cyclopalladation process (Scheme 1C, Path A) rather than the hydropalladation process (Scheme 1C, Path B), wherein the bidentate phosphine ligand is crucial to the successful realization of the transformation.

RESULTS AND DISCUSSION

At the outset, the phenylacetylene, due to its availability and the facile derivatization of desired product, was selected as a model substrate to react with CO_2. Considering the importance of ligand on the desired hydrocarboxylation reaction, a screening of bidentate-type phosphine ligands with $Pd(PPh_3)_4$ as catalyst and $PhSiH_3$ as the reductant were first examined in the presence of NEt_3 as the base (Table 1). Bidentate-type ligands with varying bite angles, including dpp-benzene, dppe, dppp, dppb, binap, DPEphos and xantphos, were investigated respectively. We were delighted to find that binap was the most suitable phosphine ligand, affording the desired product **2a** in 86% yield (entry 5). And no Pd black was observed during the transformation, indicating the high activity of the catalysis system. The use of dppp and dppb based catalysts led to decreased yields (entries 3-4), While dpp-benzene, dppe and DPEphos exhibited extremely low reactivity due to the formation of Pd black during the reaction (entries 1-2, 6). Moreover, xantphos gave no trace of the desired product but led to the generation of hydrogenation byproduct **3a** (entry 7). These results revealed the steric hindrance effect of bidentate phosphine ligands

Table 1. Optimization of the hydrocarboxylation of phenylacetylene (**1a**) with CO_2.[a]

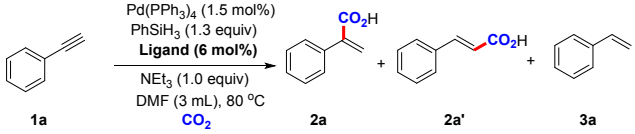

Entry	Ligand	Conversion [%]	Yield [%] [b]		
			2a	**2a'**	**3a**
1	dpp-benzene	55	trace	n.d	9
2	dppe	83	25	5	18
3	dppp	90	61	trace	trace
4	dppb	85	63	8	trace
5	binap	100	86(82)	trace	7
6	DPEphos	57	22	n.d	trace
7	Xantphos	100	n.d	n.d	49

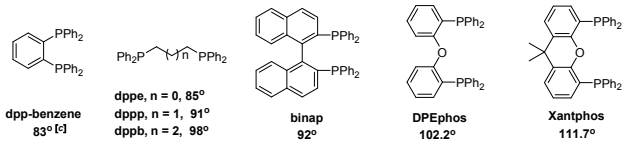

[a] Reaction conditions: **1a** (0.6 mmol), $Pd(PPh_3)_4$ (1.5 mol%), ligand (1.5 mol%), NEt_3 (1 equiv.), $PhSiH_3$ (1.3 equiv.), DMF (3 mL), CO_2 (2 MPa), 12 h. [b] NMR yield with CH_2Br_2 as the

internal standard; the number in parentheses is the yield of the isolated yield. [c] Reference 13, standardized P-M-P angles from X-ray structures and calculations.

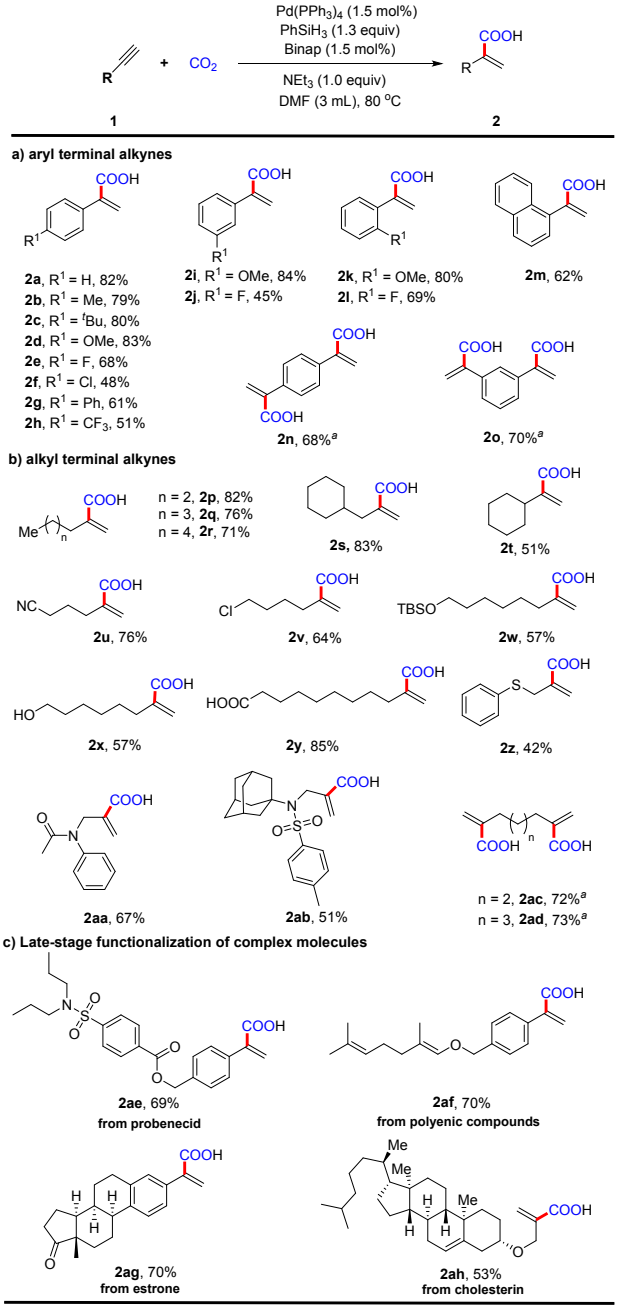

Scheme 2. Hydrocarboxylation of terminal alkynes with CO_2. Reaction conditions: **1** (0.6 mmol), $Pd(PPh_3)_4$ (1.5 mol%), binap (1.5 mol%), NEt_3 (1 equiv.), $PhSiH_3$ (1.3 equiv.), DMF (3 mL), CO_2 (2 MPa), 12 h, isolated yield. [a] Reaction conditions: **1** (0.6 mmol), $Pd(PPh_3)_4$ (3.0 mol%), binap (3.0 mol%), NEt_3 (2 equiv.), $PhSiH_3$ (2.6 equiv), DMF (3 mL), CO_2 (2 MPa), 24 h, isolated yield.

reflected by the bite angle had a rather determinative effect on the reactivity of the catalyst[13]. Moreover, control experiment showed that when the reaction was conducted in the absence of Et_3N under otherwise identical conditions, the desired product was obtained in a lower yield (Table S1, entry 23), indicating that Et_3N played an important role for the transformation.[14]

With the optimized reaction conditions in hand, our attention then turned to examine the hydrocarboxylation of terminal alkynes containing different functional groups and steric environments (Scheme 2). Gratifyingly, both electron-donating and electron-withdrawing group substituted aryl alkynes were well tolerated, giving the corresponding *α*-acrylic acids in moderate to excellent yields with excellent regioselectivity (**2a-2m**). Notably, the electronic nature of the substituents has significant influence on the product yields. Aryl alkynes with electron-withdrawing groups gave the corresponding products in lower yields than those with electron-donating groups, and styrenes were observed as the major by-products. Moreover, *meta*- and *ortho*-substituted substrates also could be successfully applied to this protocol (**2i-2l**). Interestingly, the reaction of diynes (**1n-1o**) also proceeded well but required longer reaction times and a larger amount of catalyst and reductant. Subsequently, aliphatic terminal alkynes with different chain lengths were found to be tolerated, giving the corresponding products in high yields (**2p-2r**). 2-Cyclohexylacrylic acid **2t** could be obtained a lower yield than that of **2s**, which might be attributed to the influence of steric hindrance. More importantly, various functional groups, such as cyano, chloro, silyl ethers, hydroxyl and carboxyl appended to the alkyl chain were all compatible with the standard reaction conditions, allowing for efficient synthesis of *α*-alkyl acrylic acids in high yields and excellent selectivity (**2u- 2y**). It is worth mentioning that phenyl propargyl sulfide (**1z**) could also be employed in the hydrocarboxylation transformation, albeit with moderate yield, and a large amount of allyl(phenyl)sulfane was formed as the by-product. Propynylamine protected by varied aromatic substituents or aliphatic substituents, including acetyl, phenyl, adamantly and tosyl, proceeded smoothly under the standard conditions, yielding the corresponding products **2aa-2ab** in good yields, which are difficult to prepare by other methods and could be further transformed to *β*-amino acids. Dialkyl carboxylic acid **2ac** and **2ad** were synthesized with similar efficiency and selectivity. Interestingly, high yields and regioselectivities were observed for the alkynes

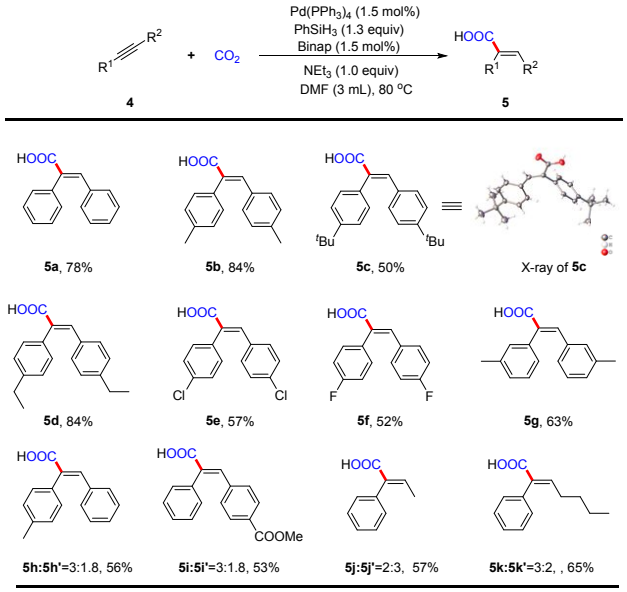

Scheme 3. Hydrocarboxylation of internal alkynes with CO_2. Reaction conditions: **4** (0.6 mmol), $Pd(PPh_3)_4$ (1.5 mol%), binap (1.5 mol%), NEt_3 (1 equiv.), $PhSiH_3$ (1.3 equiv.), DMF (3 mL), CO_2 (2 MPa), 12 h, isolated yield.

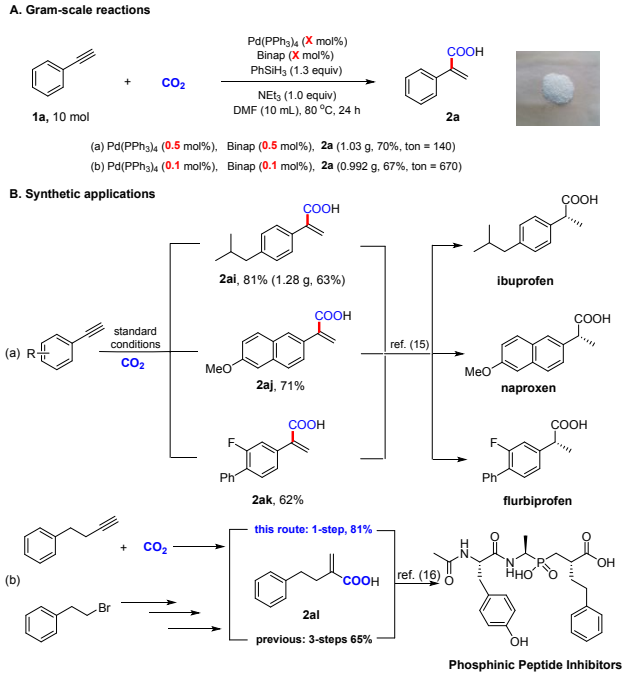

Scheme 4. Gram-scale reactions and synthetic applications.

derived from the modifications of drug molecules and natural products, such as probenecid (**2ae**), estrone (**2ag**), cholesterol (**2ah**), despite the fact that the starting alkynes contained ketones, alkenes, and ethers functionalities, offering a potential strategy for the late-stage functionalization of alkyne-containing complex natural products and pharmaceuticals.

To further explore the utilities of our method, the substrate scope was extended to different internal alkynes **4** (Scheme 3). As expected, various symmetrical diarylalkynes (**4a**-**4g**) containing electron-donating and electron-withdrawing substituents such as methyl, ethyl, *t*-butyl, fluoro, chloro, were all tolerated under the reaction conditions, delivering the corresponding (*E*)-2,3-diarylacrylic acids as the sole products in moderate to high yields. Similarly, electron-donating substituted diarylacetylenes gave the corresponding products in higher yields than those with electron-withdrawing substituents (**5a**-**5f**). The structure of product **5c** was characterized unambiguously by X-ray crystallographic analysis.[15] For unsymmetrical alkynes, diarylalkynes (**4h**-**4i**) with a *para*-substituent on one of the phenyl rings afforded a mixture of products in moderate yield, wherein CO_2 insertion took place predominantly adjacent to the electron-rich site. For 1-phenyl-1-propyne **4j**, the carboxylation tended to occur at the carbon atom near the alkyl group to produce the vinyl carboxylic acids in 57% combined yield, but for substrate **4k**, the reaction underwent with the opposite selectivity pattern. It should be pointed out that, in these two cases, large amounts of the starting materials could be recovered unchanged.

To further illustrate the value of this unique Pd-catalyzed hydrocarboxylation reaction, we applied it in the synthesis of biologically active compounds (Scheme 4). Firstly, a gram-scale (10 mmol) experiment was successfully conducted to deliver the product **2a** with 70% isolated yield

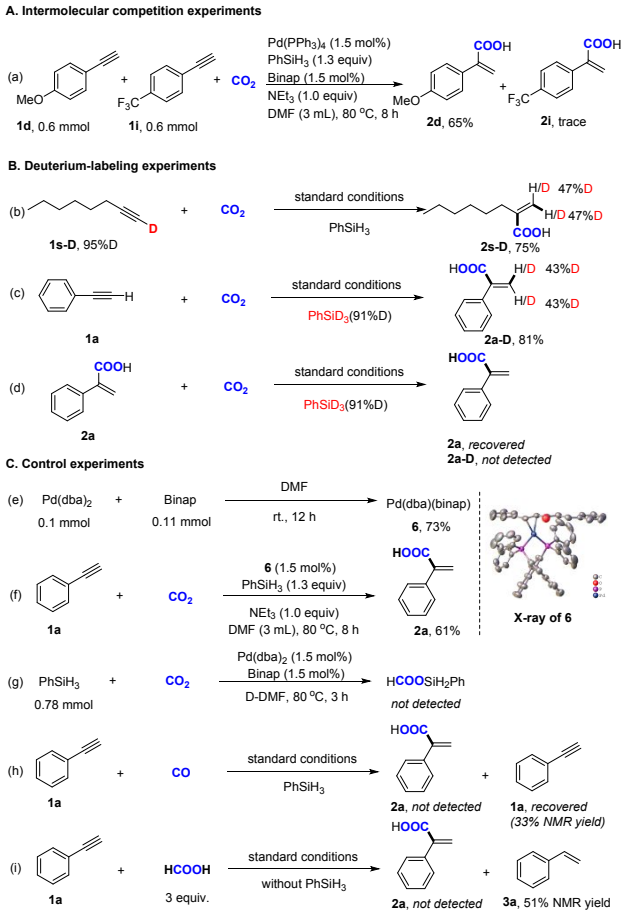

Scheme 5. Intermolecular competition experiments and mechanistic studies.

in high selectivity by employing 0.5 mol% $Pd(PPh_3)_4$ and 0.5 mol% Binap. Pleasingly, reducing the amount of catalyst to 0.1 mol%, this transformation could proceed smoothly without the significant erosion in yield and regioselectivity,

which demonstrated the high-efficiency of this catalytic system in hydrocarboxylation of alkynes and CO_2 (Scheme 4A). Subsequently, α-acrylic acids **2ai, 2aj**, **2ak** could be synthesized by our protocol in high yields, which are important synthetic intermediates for the preparation of ibuprofen, naproxen and flurbiprofen, nonsteroidal anti-inflammatory drugs, respectively (Scheme 4B, a).[16] Moreover, the product **2al**, a key intermediate for the synthesis of the phosphinic peptide inhibitor,[17] could be prepared by our catalytic approach in a high yield, while previously reported method involved three steps with (2-bromoethyl)benzene as the starting material in only 65% yield. (Scheme 4B, b). These examples illustrated this catalytic protocol could provide an effective tool for the preparation of pharmaceuticals containing a carboxylic acid functional group.

To get a deeper understanding of the reaction, some mechanistic studies were conducted. Firstly, an intermolecular competition experiment with the mixture of electron-rich and electron-deficient alkynes as substrates was carried out under the standard conditions (Scheme 5A). The reaction afforded the product **2d** with 65% yield and gave a trace amount of the product **2i**, which indicated electron-rich substrates were

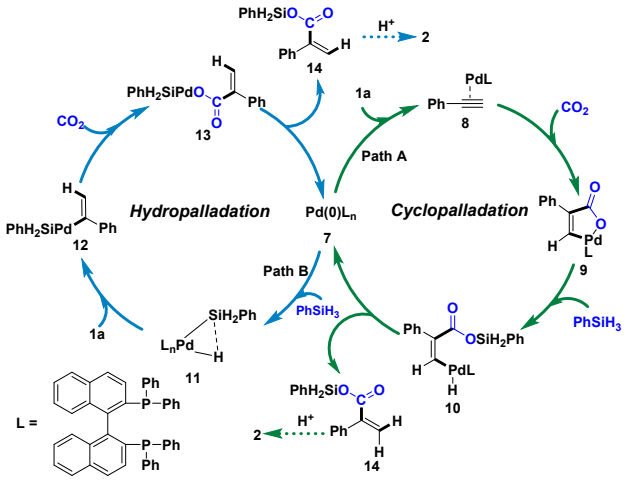

Scheme 6. Proposed reaction mechanism.

more favourable for this Pd-catalyzed hydrocarboxylation reaction. Then, deuterium labelling experiments were performed. Both the hydrocarboxylation of **1r-D** with $PhSiH_3$ and **1a** with $PhSiD_3$ furnished deuterated targeted products with an *E*/*Z* ratio of 1:1 (Scheme 5B, b and c). We speculated the reason might be due to the intramolecular H/D exchange of the product during the extraction process in the presence of protonic acid, which have been demonstrated in Scheme S3. In addition, in order to exclude the direct H/D exchange possibility of product **2a** with $PhSiD_3$, the product **2a** was used as substrate to react with $PhSiD_3$ under the standard conditions (Scheme 5B, d). These results demonstrated $PhSiH_3$ might serve as proton donor in this Pd-catalyzed hydrocarboxylation reaction. Moreover, we observed the formation of the active Pd catalyst upon the reaction, which was generated in situ from Pd reagents and Binap. Employing the active Pd catalyst **6** as catalyst, which was prepared from $Pd(dba)_2$ and Binap, the reaction afforded the product **2a** with 61% yield (Scheme 5C, f). The structure of **6** was confirmed unambiguously by X-ray crystallography.[18] To further study the mechanism, the reaction of CO_2 with hydrosilane in the presence of Pd catalyst was conducted. However, no desired silyl formate product was detected, which suggested that silyl formates might not be key intermediates for the transformation (Scheme 5C, g).[19] Furthermore, in order to exclude the possibility of HCOOH or CO as the intermediate, derived from the reduction of CO_2 in the presence of $PhSiH_3$, two control experiments were designed. Replacing CO_2 with CO under the standard conditions, the product **2a** could not be detected together with the formation of by-product **3a** (Scheme 5C, h). Additionally, Employing HCOOH as substrate to react with phenylacetylene without the $PhSiH_3$, the reaction provided no product **2a**, wherein **3a** and 1,3-butadiene were as the major by-products (Scheme 5C, i). Therefore, these observations excluded the involvement of the CO or HCOOH process.

On the basis of the experimental results, as well as previous reports[7b, 9f, 20], plausible mechanistic pathways for the hydrocarboxylation were tentatively proposed in Scheme 6. Firstly, the active palladium catalyst **7** was generated in situ from palladium catalyst and Binap. Subsequently, the reaction might proceed *via* the oxidative cyclization process to afford five-membered palladiumalactone intermediate **9** (Scheme 6, Path A), which could react with $PhSiH_3$ to produce intermediate **10**. Then, intermediate **10** underwent the reductive elimination to afford intermediate **14** and regenerate the Pd(0)L species **7**. Finally, the desired product **2a** was released from intermediate **14** in the presence of protonic acid together with the formation of the derivatives of silane.[7b, 20a] Additionally, the reaction also might proceed the hydropalladation process in the presence of $PhSiH_3$ and binap, giving the alkenylpalladium intermediate **12** (Scheme 6, Path B). Then, the insertion of CO_2 into the vinyl-Pd bond produced intermediate **13**, followed by the reductive elimination and protonolysis to afford the desired product **2a**.

To probe the nature of the regioselective hydrocarboxylation of alkynes with carbon dioxide catalyzed by Pd(0) complex, DFT calculations at ωB97X-D/BSII//ωB97X-D/BSI level were carried out on the whole catalytic cycles of Path A and Path B above shown in Scheme 6. BSI denotes that the LANL2DZ basis set is used for Pd center and the 6-31G (d) basis sets for all the other atoms, and BS Ⅱ denotes that the LANL2DZ basis sets were used for Pd center and the 6-31++G (d, p) basis sets for all the other atoms. DFT calculations at ωB97X-D/BSII//ωB97X-D/BSI level mean that single point calculations were performed at ωB97X-D/BSII level based on geometry optimization at ωB97X-D/BSI level for each stationary point along reaction pathways. The SMD polarizable continuum model in *N*, *N*-dimethylformamide as the solvent was employed in the calculations.[21] Thermal correction and entropy contribution to the Gibbs free energy were taken from the frequency calculations at ωB97X-D/BSI level. To avoid the overestimated entropic effect induced by thermal corrections from gas-phase optimization, in this study, translational movement was evaluated using the method presented by Whitesides.[22] The free energy profiles of Path A and Path B are shown in Scheme 7A and 7B,

respectively. Path A consists of four fundamental steps: the coordination of phenylacetylene, the cyclopalladation step, the *σ*-bond metathesis step and the reductive elimination step. Similarly, Path B consists of four steps: the oxidative addition step, the phenylacetylene insertion step, the CO_2 insertion step and the reductive elimination step. Path A1/B1 and Path A2/B2 represent the Markovnikov addition pathway and anti-Markovnikov addition pathway, respectively. The difference between Path A and Path B is in the insertion sequence of substrates of phenylacetylene, CO_2 and silane.

In Path A, phenylacetylene coordinates with Pd center of the catalytic species (**7**) to form **8** at first, which is exothermic by 22.7 kcal/mol (Scheme 7A). Then O^1 of CO_2 approaches to Pd center of **8** and C^3 interacts with C^2 of coordinated phenylacetylene in the cyclopalladation step, which give intermediates $\mathbf{9^{A1}}$ owning a five-membered ring *via* the transition state $\mathbf{TS8\text{-}9^{A1}}$ along Markovnikov addition route and $\mathbf{9^{A2}}$ via $\mathbf{TS8\text{-}9^{A2}}$ along anti-Markovnikov addition route ($\mathbf{9^{A1}}$/$\mathbf{9^{A2}}$ denotes stationary point **9** along Path A1/A2). The free energy barriers of the cyclopalladation step of Path A1 and Path A2 are 11.7 kcal/mol and 13.8 kcal/mol, respectively. In the *σ*-bond metathesis step of Path A, the Pd-O^1 bond of fiver-membered ring of **9** is broken and Si-H^1 bond of substrate silane is broken *via* transition states $\mathbf{TS9\text{-}10^{A1}}$/$\mathbf{TS9\text{-}10^{A2}}$ owning a seven-membered ring moiety,

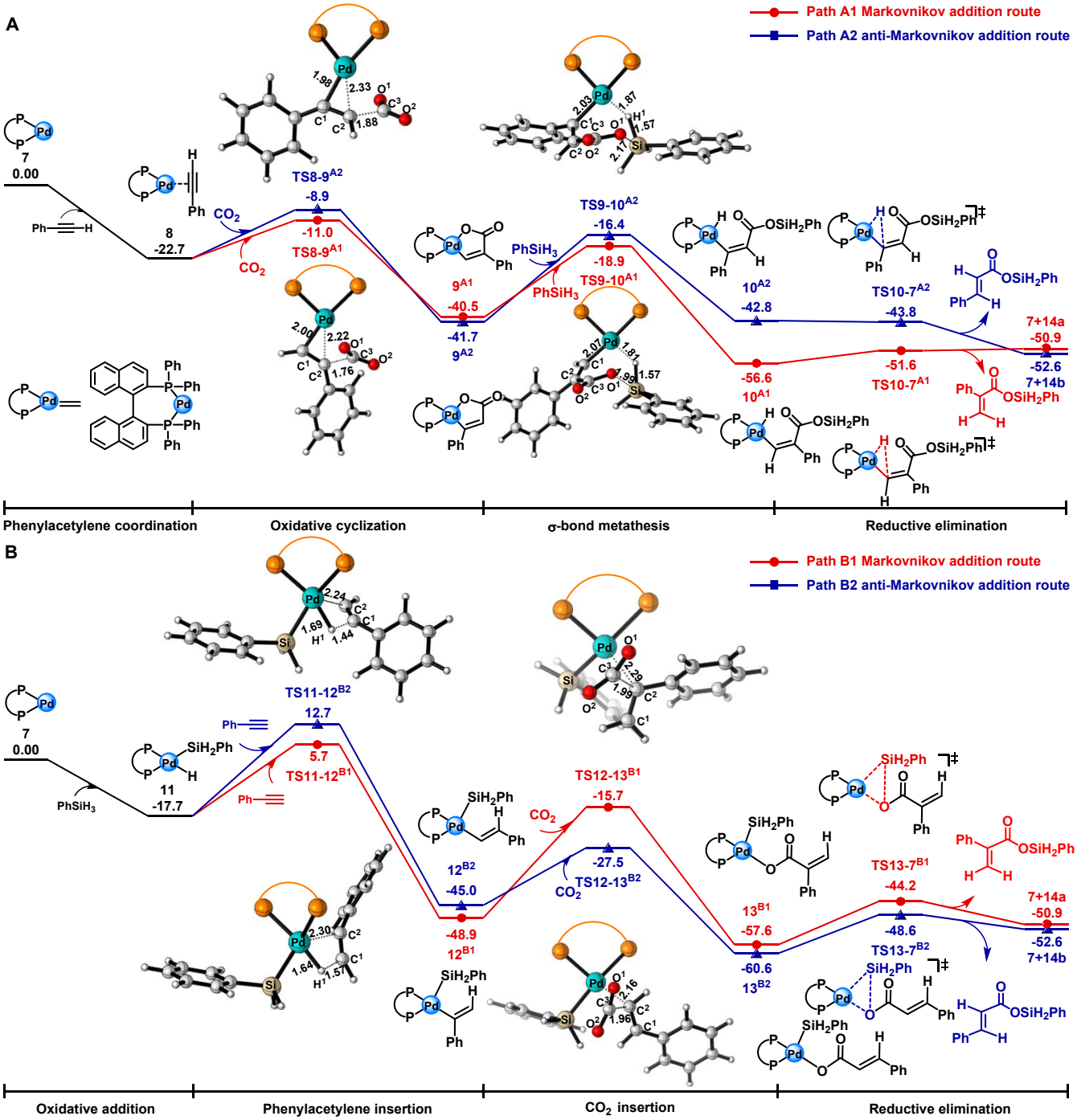

Scheme 7. The calculated relative Gibbs free energies to catalytic species (**7**) of stationary points along (A) the cyclopalladation pathway (Path A) and (B) the hydropalladation pathway (Path B) (All energies are denoted in kcal/mol, and interatomic distances are shown in Å. The blue line stands for Path A1 and Path B1 adopting Markovnikov addition mode, the red line stands for Path A2 and Path B2 adopting Anti-Markovnikov addition mode).

which form **10**^{A1}/**10**^{A2}. The free energy barriers of the *σ*-bond metathesis step from **9** to **10** of Path A1 and Path A2 are 21.6 kcal/mol and 25.3 kcal/mol, respectively. In the reductive elimination step, the hydrocarboxylated products (**14a**/**14b**) are released via transition states **TS10-7**^{A1}/**TS10-7**^{A2} and the catalytic species (**7**) are regenerated. The free energy barriers of the reductive elimination step from **10**^{A1} to **7**^{A1} for Path A1 is 5.0 kcal/mol. The process from **10**^{A2} to **TS10-7**^{A2} in Path A2 has no free energy barrier, in which the free energy of **TS10-7**^{A2} is lower than that of **10**^{A2} due to the entropy effect. Similarly, the calculated free energy barriers of the oxidative addition step, the phenylacetylene insertion step, the CO_2 insertion step and the reductive elimination step of Path B1/B2 are 0.0/0.0, 23.4/30.4, 33.2/27.5 and 13.4/12.0 kcal/mol, respectively (Scheme 7B). It is obvious that Path A *via* cyclopalladation is more favorable than Path B *via* hydropalladation. The rate-determining step of Path A1 and Path A2 is the *σ*-bond metathesis process, and the rate-

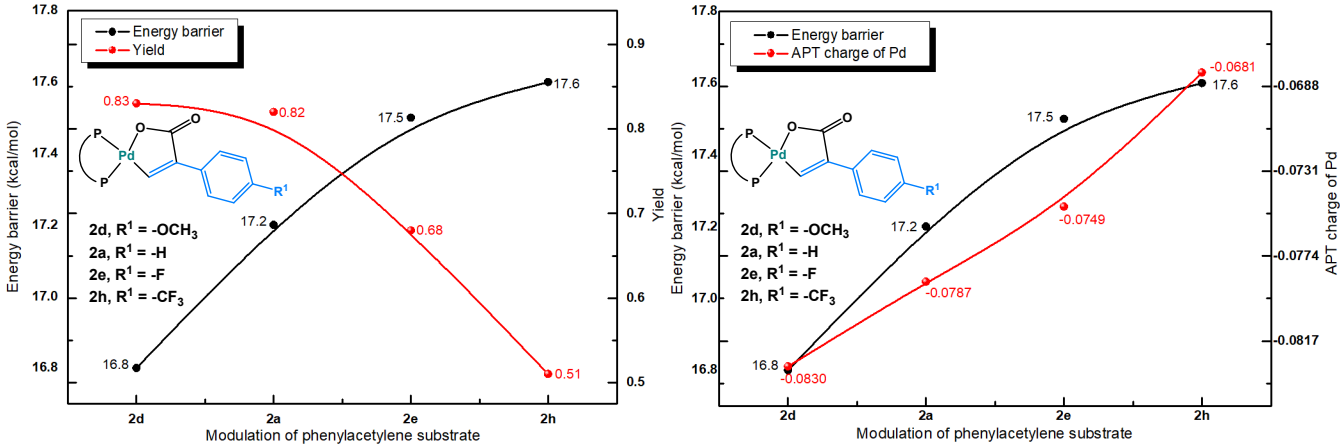

Scheme 8. The relationship of the free energy barriers (at ωB97X-D/BSI level) of the rate-determining step (the *σ*-bond metathesis) in Path A1 and different substrates (the black line), and that of the experimental yields and different substrates/APT charge (the red line) (different substrates in *para*-position of phenyl ring were subsitituted by -OCH_3 (**2d**), -H (**2a**), -F (**2e**), and -CF_3 (**2h**), respectively).

determining step of Path B1 and Path B2 are the CO_2 insertion step and the phenylacetylene insertion step, respectively. On the other hand, Markovnikov addition along Path A1 is more favorable than anti-Markovnikov addition along Path A2. In general, the carboxylation of phenylacetylene catalyzed by Pd complex adopts oxidative cyclization pathway with Markovnikov addition mode (Path A1). The carboxylation products observed in the experiments are mainly Markovnikov products, and the calculated results agree well with experiments.

In the rate-determining step of Path A, the *σ*-bond metathesis step, Pd-H^1 bond and Si-O^1 bond of **9** are formed while Pd-O^1 bond is broken. Interestingly, the calculated ∠ Pd-O^1-C^3-O^2 dihedral angles change from 179°/174° in $\mathbf{9^{A1}}$/$\mathbf{9^{A2}}$ to 145°/127° in $\mathbf{TS9\text{-}10^{A1}}$/$\mathbf{TS9\text{-}10^{A2}}$, respectively. The Pd-$O^1$-$C^3$-$O^2$ dihedral angle in the *σ*-bond metathesis step of Path A2 changed larger than that of Path A1, which could be in that the steric effect of phenyl part of the original phenylacetylene in anti-Markovnikov addition (Path A2) destroy the conjugation of C^1=C^2 double bond, C^3=O^2 double bond and phenyl ring. As a result, the energy barrier of is the *σ*-bond metathesis step of Path A1 following Markovnikov addition is lower than that of Path A2 following anti-Markovnikov addition. Based on APT charge analysis,[23] the phenyl ring in phenylacetylene has a pull electron effect on the C-C triple bond, the APT charges of Pd in $\mathbf{9^{A1}}$ and $\mathbf{9^{A2}}$ are -0.079 and -0.013, respectively. Compared with that of $\mathbf{9^{A1}}$, the phenyl moiety of $\mathbf{9^{A2}}$ has a stronger pull electron effect on the Pd center. These are consistent with the calculated free energy barriers of the *σ*-bond metathesis step and the reductive elimination step in Path A1 and Path A2, which may unveil the nature of preference of Markovnikov addition.

In order to further understand the substituent effect of substrates on the reaction, we substituted the *para*-position of phenyl ring of $\mathbf{9^{A1}}$ using electron-donating group (-OCH_3) and the electron-withdrawing groups (-F, -CF_3) in the rate-determining step (the *σ*-bond metathesis step) of Path A1 adopting Markovnikov addition mode. As shown in Scheme 8, the calculated free energy barriers of this step of the reaction using substrates in *para*-position of phenyl ring subsitituted by -OCH_3 (**2d**), -H (**2a**), -F (**2e**), and -CF_3 (**2h**) were 16.8, 17.2, 17.5, 17.6 kcal/mol, respectively. The calculated results agree well with experimental yields present in Scheme 2 above. Meanwhile, the calculated free energy barriers of the rate-determining step of different phenylacetylene substrate and the APT charges of Pd center are positively correlated, this implies that the electron-withdrawing group in *para*-position of benzene ring of phenyl alkyne substates could increase positivity of Pd center, leading to a decrease in reactivity. In other words, the alkyne substrates with stronger electron-donating ability could promote the reaction.

In addition, the phosphorus ligand effect of Pd catalysts was investigated by experimental and theoretical studies. The calculated bite angles of Binap, DPEphos and Xanphos are 92°, 102.2° and 111.7°, respectively. Based on the DFT calculations, the rate-determining step of DPEphos and Xanphos Pd catalytic systems changed from the *σ*-bond metathesis step to the cyclopalladation step along Path A. The free energy barriers of the cyclopalladation step for DPEphos and Xanphos Pd systems are 32.1 and 31.0 kcal/mol, respectively. These are also consistent with the experimental results. It indicates that a Pd catalyst owning larger bite angle of diphosphorus ligand debilitates its catalytic activity for this reaction.

CONCLUSION

In summary, we have developed a highly regioselective Pd-catalyzed hydrocarboxylation of alkynes with CO_2, offering an attractive route towards straightforward synthesis of various *α*-acrylic acids, a privileged motif widely existed in a number of natural products and pharmaceuticals. This catalyst system exhibited excellent catalytic activity under the mild reaction conditions. Additionally, this transformation provides a powerful tool for the late-stage functionalization of alkyne-containing complex molecules, including natural products and pharmaceuticals. A DFT study was performed to investigate the reaction mechanism. The calculated results demonstrate that the cyclopalladation (Path A) is more favorable than the hydropalladation (Path B). The rate-determining step is the *σ*-bond metathesis step owning a free energy barrier of 25.8 kcal/mol. Markovnikov addition (Path A1) is dominant compared to anti-Markovnikov addition (Path A2), which correlate well with

experiments. Further investigations to extend the substrate scope of the synthetic protocol together with detailed mechanistic investigations are ongoing in our laboratory.

ASSOCIATED CONTENT

Supporting Information

The Supporting Information is available free of charge on the ACS Publications website at http://pubs.acs.org.
Experimental procedures, detailed condition screening table, characterization data, and copies of NMR spectra for all products (PDF)

AUTHOR INFORMATION

Corresponding Author

crqi@scut.edu.cn

leim@mail.buct.edu.cn

jianghf@scut.edu.cn

Author Contributions

ORCID

Notes
The authors declare no competing financial interests.

ACKNOWLEDGMENT

This work was supported by the Ministry of Science and Technology of the People's Republic of China (2016YFA0602900), the National Natural Science Foundation of China (21971073 and 21672018) and the Guangdong Natural Science Foundation (2019A1515011468 and 2017A030313054), China Postdoctoral Science Foundation (2018M640774) and the Fundamental Research Funds for the Central Universities (D2191970 and D2190580) for financial support.

REFERENE

(1) (a) Kanno, K.; Igarashi, E.; Zhou, L.; Nakajima, K.; and Takahashi, T. Selective Linear Triene Formation from Different Alkynes using Zr/Cu system. *J. Am. Chem. Soc.* **2008**, *130*, 5624–5625. (b) Ding, S.; Song, L.-J.; Chung, L. W.; Zhang, X.; Sun, J.; Wu, Y.-D. Ligand-Controlled Remarkable Regio- and Stereodivergence in Intermolecular Hydrosilylation of Internal Alkynes: Experimental and Theoretical Studies. *J. Am. Chem. Soc.* **2013**, *135*, 13835−13842. (c) Fang, G.; Bi, X. Silver-catalysed Reactions of Alkynes: Recent Advances. *Chem. Soc. Rev.* **2015**, *44*, 8124–8173. (d) Guo, J.; Shen, X.; Lu, Z. Regio- and Enantioselective Cobalt-Catalyzed Sequential Hydrosilylation/Hydrogenation of Terminal Alkynes. *Angew. Chem. Int. Ed.* **2017**, *56*, 615–618. (e) Yang, J.-M.; Zhao, Y.-T.; Li, Z.-Q.; Gu, X.-S. Zhu, S.-F.; Zhou, Q.-L. Gold-Catalyzed Oxidative Coupling of Terminal Alkynes and Borane Adducts: Efficient Synthesis of α-Boryl Ketones. *ACS Catal.* **2018**, *8*, 7351−7355. (f) Zhang, Z.-Q.; Zheng, M.-M.; Xue, X.-S.; Marek, I.; Zhang, F.-G.; Ma, J.-A. Catalytic Enantioselective Cyclopropenation of InternalAlkynes: Access to Difluoromethylated Three-Membered Carbocycles. *Angew. Chem. Int. Ed*. **2019**, *58*, 18191–18196. (g) Hu, M.-Y.; Lian, J.; Sun, W.; Qiao, T.-Z.; Zhu, S.-F. Iron-Catalyzed Dihydrosilylation of Alkynes: Efficient Access to Geminal Bis(silanes). *J. Am. Chem. Soc*. **2019**, *141*, 4579−4583. (h) Song, C.; Dong, X.; Wang, Z.; Liu, K.; Chiang, C.-W.; Lei, A. Visible-Light-Induced [4+2] Annulation of Thiophenes and Alkynes to Construct Benzene Rings. *Angew. Chem. Int. Ed*. **2019**, *58*, 12206–12210. (i) Song, L.; Feng, Q.; Wang, Y.; Ding, S.; Wu, Y.-D.; Zhang, X.; Chung, L. W.; Sun, J. Ru-Catalyzed Migratory Geminal Semihydrogenation of Internal Alkynes to Terminal Olefins. *J. Am. Chem. Soc*. **2019**, *141*, 17441−17451.

(2) (a) Wang, P.; Yeo, X.-L.; Loh, T.-P. Copper-Catalyzed Highly Regioselective Silylcupration of Terminal Alkynes to Form α-Vinylsilanes. *J. Am. Chem. Soc.* **2011**, *133*, 1254–1256. (b) Manan, R. S.; Kilaru, P.; Zhao, P. Nickel-Catalyzed Hydroimination of Alkynes. *J. Am. Chem. Soc.* **2015**, *137*, 6136−6139. (c) Obligacion, J. V.; Neely, J. M.; Yazdani, A. N.; Pappas, I.; Chirik, P. J. Cobalt Catalyzed *Z*-Selective Hydroboration of Terminal Alkynes and Elucidation of the Origin of Selectivity. *J. Am. Chem. Soc*. **2015**, *137*, 5855−5858. (d) Guo, J.; Lu, Z. Highly Chemo-, Regio-, and Stereoselective Cobalt-Catalyzed Markovnikov Hydrosilylation of Alkynes. *Angew. Chem. Int. Ed.* **2016**, *55*, 10835–10838. (e) Ye, F.; Chen, J.; Ritter, T. Rh-Catalyzed Anti-Markovnikov Hydrocyanation of Terminal Alkynes. *J. Am. Chem. Soc.* **2017**, *139*, 7184−7187. (f) Yang, X.; Wang, C. Dichotomy of Manganese Catalysis via Organometallic or Radical Mechanism: Stereodivergent Hydrosilylation of Alkynes. *Angew. Chem. Int. Ed.* **2018**, *57*, 923–928. (g) Chen, T.; Zhao, C.-Q.; Han, L.-B. Hydrophosphorylation of Alkynes Catalyzed by Palladium: Generality and Mechanism. *J. Am. Chem. Soc*. **2018**, *140*, 3139−3155. (h) Wu, C.; Teo, W. J.; Ge, S. Cobalt-Catalyzed (*E*)-Selective anti-Markovnikov Hydrosilylation of Terminal Alkynes. *ACS Catal*. **2018**, *8*, 5896−5900. **(**i) Lee, M. T.; Goodstein, M. B.; Lalic, G. Synthesis of Isomerically Pure (*Z*)-Alkenes from Terminal Alkynes and Terminal Alkenes: Silver-Catalyzed Hydroalkylation of Alkynes. *J. Am. Chem. Soc*. **2019**, *141*, 17086−17091. (j) Alami, M.; Hamze, A.; Provot, O. Hydrostannation of Alkynes. *ACS Catal*. **2019**, *9*, 3437−3466. (k) Yu, P.; Bismuto, A.; Morandi, B. Iridium-Catalyzed Hydrochlorination and Hydrobromination of Alkynes via Shuttle Catalysis. *Angew. Chem. Int. Ed*. **2020**, *59*, 2904 –2910.

(3) For selected reviews: (a) Huang, K.; Sun, C.-L.; Shi, Z.-J. Transition-metal-catalyzed C–C Bond Formation through The Fixation of Carbon Dioxide. *Chem. Soc. Rev.* **2011**, *40*, 2435–2452. (b) Zhang, L.; Hou, Z. N-Heterocyclic Carbene (NHC)–Copper-catalysed Transformations of Carbon Dioxide. *Chem. Sci.* **2013**, *4*, 3395–3403. (c) Yu, D.; Teong, S.; Zhang, Y. Transition Metal Complex Catalyzed Carboxylation Reactions with CO_2. *Coord. Chem. Rev*. **2015**, *293–294*, 279–291. (d) Song, Q.-W.; Zhou, Z.-H.; He, L.-N. Efficient, Selective and Sustainable Catalysis of Carbon Dioxide. *Green Chem.* **2017**, *19*, 3707–3728. (e) Sun, Z.; Ma, T.; Tao, H.; Fan, Q.; Han, B. Fundamentals and Challenges

of Electrochemical CO_2 Reduction Using Two-Dimensional Materials *Chem*, **2017**, *3*, 560–587. (f) Tortajada, A.; Juliá-Hernández, F.; Börjesson, M.; Moragas, T.; Martin, R. Transition-Metal-Catalyzed Carboxylation Reactions with Carbon Dioxide. *Angew. Chem. Int. Ed.* **2018**, *57*, 15948–15982. (g) Yan, S.-S.; Fu, Q.; Liao, L.-L.; Sun, G.-Q.; Ye, J.-H.; Gong, L.; Bo-Xue, Y.-Z.; Yu, D.-G. Transition Metal-catalyzed Carboxylation of Unsaturated Substrates with CO_2. *Coord. Chem. Rev*. **2018**, *374*, 439−463; For selected papers: (h) Manjolinho, F.; Arndt, M.; Gooßen, K.; Gooßen, L. J. Catalytic C−H Carboxylation of Terminal Alkynes with Carbon Dioxide. *ACS Catal*. **2012**, *2*, 2014−2021. (i) Tran-Vu, H.; Daugulis, O. Copper-Catalyzed Carboxylation of Aryl Iodides with Carbon Dioxide. *ACS Catal*. **2013**, *3*, 2417−2420. (j) Ma, C.; Zhao, C.-Q.; Xu, X.-T.; Li, Z.-M.; Wang, X.-Y.; Zhang, K.; Mei, T.-S. Nickel-Catalyzed Carboxylation of Aryl and Heteroaryl Fluorosulfates Using Carbon Dioxide. *Org. Lett*. **2019**, *21*, 2464−2467. (k) Li, Z.; Zhang, L.; Nishiura, M.; Luo, G.; Luo, Y.; Hou, Z. CO_2 Activation by Lewis Pairs Generated Under Copper Catalysis Enables Difunctionalization of Imines. *J. Am. Chem. Soc*. **2020**, *142*, 1966–1974.

(4) (a) Wenzel S. C.; Bode, H. B. Novel Polyene Carboxylic Acids from Streptomyces. *J. Nat. Prod*. **2004**, *67*, 1631-1633. (b) Yang, R.; Yang, J.; Wang, L.; Huang, J.-P.; Xiong, Z.; Luo, J.; Yu, M.; Yan, Y.; Huang, S.-X. Lorneic Acid Analogues from an Endophytic Actinomycete. *J. Nat. Prod.* **2017**, *80*, 2615−2619. (c) Chepkirui, C.; Yuyama, K. T.; Wanga, L. A.; Decock, C.; Matasyoh, J. C.; Abraham, W.-R.; Stadler, M. Microporenic Acids A–G, Biofilm Inhibitors, and Antimicrobial Agents from the Basidiomycete Microporus Species. *J. Nat. Prod*. **2018**, *81*, 778−784. (d) Lesma, G.; Luraghi, A.; Bavaro, T.; Bortolozzi, R.; Rainoldi, G.; Roda, G.; Viola, G.; Ubiali, D.; Silvani, A. Phytosterol and *γ*-Oryzanol Conjugates: Synthesis and Evaluation of their Antioxidant, Antiproliferative, and Anticholesterol Activities. *J. Nat. Prod.* **2018**, *81*, 2212−2221.

(5) (a) Viegas, A.; Manso, J.; Corvo, M. C.; Marques, M. M. B.; Cabrita, E. J. Binding of Ibuprofen, Ketorolac, and Diclofenac to COX-1 and COX-2 Studied by Saturation Transfer Difference NMR. *J. Med. Chem*. **2011**, *54*, 8555−8662. (b) Srivastava, S. K.; Ramana, K. V. Encyclopedia of Cancer: Nonsteroidal Anti-inflammatory Drugs, Springer-Verlag Berlin Heidelberg, **2015**, 1−4. (c) Gurney, M. E.; Nugent, R. A.; Mo, X.; Sindac, J. A.; Hagen, T. J.; Fox, III, D.; O 'Donnell, J. M.; Zhang, C.; Xu, Y.; Zhang, H.-T.; Groppi, V. E.; Bailie, M.; White, R. E.; Romero, D. L.; Vellekoop, A. S.; Walker, J. R.; Surman, M. D.; Zhu, L.; Campbell, R. F. Design and Synthesis of Selective Phosphodiesterase 4D (PDE4D) Allosteric Inhibitors for the Treatment of Fragile X Syndrome and Other Brain Disorders. *J. Med. Chem*. **2019**, *62*, 4884−4901. (d) Findlay, A. D.; Foot, J. S.; Buson, A.; Deodhar, M.; Jarnicki, A. G.; Hansbro, P. M.; Liu, G.; Schilter, H.; Turner, C. I.; Zhou, W.; Jarolimek, W. Identification and Optimization of Mechanism-Based Fluoroallylamine Inhibitors of Lysyl Oxidase-like 2/3. *J. Med. Chem*. **2019**, *62*, 9874−9889.

(6) (a) Burkhart, G.; Hoberg, H. Oxanickelacyclopentene Derivatives from Nickel(o), Carbon Dioxide, and Alkynes. *Angew. Chem. Int. Ed. Etigl*. **1982**, *21*, 1. (b) Saito, S.; Nakagawa, S.; Koizumi, T.; Hirayama, K.; Yamamoto, Y. Nickel-Mediated Regio- and Chemoselective Carboxylation of Alkynes in the Presence of Carbon Dioxide. *J. Org. Chem.* **1999**, *64*, 3975–3978. (c) Aoki, M.; Kaneko, M.; Izumi, S.; Ukai, K.; Iwasawa, N. Bidentate Amidine Ligands for Nickel(0)-mediated Coupling of Carbon Dioxide with Unsaturated Hydrocarbons. *Chem. Commun*. **2004**, 2568–2569. (d) Saito, N.; Abdullah, I.; Hayashi, K.; Hamada, K.; Koyama, M.; Sato, Y. Enantioselective synthesis of *β*-amino acid derivatives via nickel-promoted regioselective carboxylation of ynamides and rhodium-catalyzed asymmetric hydrogenation. *Org. Biomol. Chem*. **2016**, *14*, 10080–10089.

(7) (a) Li, S.; Yuan, W.; Ma, S. Copper-Catalyzed Hydrocarboxylation of Alkynes Using Carbon Dioxide and Hydrosilanes. *Angew. Chem. Int. Ed*. **2011**, *50*, 2578–2582. (b) Fujihara, T.; Xu, T.; Semba, K.; Terao, J.; Tsuji, Y. Highly Regio- and Stereoselective Three-Component Nickel-Catalyzed syn-Hydrocarboxylation of Alkynes with Diethyl Zinc and Carbon Dioxide. *Angew. Chem. Int. Ed.* **2011**, *50*, 523–527. (c) Wang, X.; Nakajima, M.; Martin, R. Ni-Catalyzed Regioselective Hydrocarboxylation of Alkynes with CO_2 by Using Simple Alcohols as Proton Sources. *J. Am. Chem. Soc*. **2015**, *137*, 8924−8927. (d) Santhoshkumar, R.; Hong, Y.-C.; Luo, C,-Z.; Wu, Y.-C.; Hung, C.-H.; Hwang, K.-Y. A.-P. Tu, and C.-H. Cheng, Synthesis of Vinyl Carboxylic Acids using Carbon Dioxide as a Carbon Source by Iron-Catalyzed Hydromagnesiation. *ChemCatChem*, **2016**, *8*, 2210–2213. (e) Doi, R.; Abdullah, I.; Taniguchi, T.; Saito, N. Sato, Y. Nickel-catalyzed Hydrocarboxylation of Ynamides with CO_2 and H_2O: Observation of Unexpected Regioselectivity. *Chem. Commun*. **2017**, *53*, 7720-7723. (f) Gaydou, M.; Moragas, T.; Juliá-Hernández, F.; Martin, R. Site-Selective Catalytic Carboxylation of Unsaturated Hydrocarbons with CO_2 and Water. *J. Am. Chem. Soc*. **2017**, *139*, 12161−12164.

(8) (a) Tsuji, J. Palladium Reagents and Catalysts Innovations in Organic Synthesis. John Wiley & Sons, Inc., England, **1995**. (b) Negishi, E. Handbook of Organopalladium Chemistry for Organic Synthesis. John Wiley & Sons, Inc., New York, **2002**.

(9) (a) Sasaki, Y.; Inove, Y.; Hashimoto, H. Reaction of Carbon Dioxide with Butadiene Catalysed by Palladium Complexes. Synthesis of 2-Ethylidenehept -5-en-4-olide. *J. Chem. Soc. Chem. Commun*. **1976**, 605. (b) Sakamoto, M.; Shimizu, I.; Yamamoto, A. Synthesis of the First Carbon Dioxide Coordinated Palladium(0) Complex, $Pd(\eta^2\text{-}CO_2)(PMePh_2)_2$. *Organometallics* **1994**, *13*, 407−409. (c) Johansson, R.; Wendt, O. F. Insertion of CO_2 into a Palladium Allyl Bond and a Pd(II) Catalysed Carboxylation of Allyl Stannanes. *Dalton Trans*. **2007**, 488−492. (d) Yeung, C. S.; Dong, V. M. Beyond Aresta's Complex: Ni- and Pd-Catalyzed Organozinc

Coupling with CO_2. *J. Am. Chem. Soc.* **2008**, *130*, 7826–7827. (e) Sasano, K.; Takaya, J.; Iwasawa, N. Palladium(II)-Catalyzed Direct Carboxylation of Alkenyl C−H Bonds with CO_2. *J. Am. Chem. Soc*. **2013**, *135*, 10954−10957. (f) Manzini, S.; Cadu, A.; Schmidt, A.-C.; Huguet, N.; Trapp, O.; Paciello, R.; Schaub, T. Enhanced Activity and Recyclability of Palladium Complexes in the Catalytic Synthesis of Codium Acrylate from CO_2 and Ethylene. *ChemCatChem.* **2017**, *9*, 2269−2274. (g) Song, J.; Liu, Q.; Liu, H.; Jiang, X. Recent Advances in Palladium-Catalyzed Carboxylation with CO_2. *Eur. J. Org. Chem*. **2018**, 696–713.

(10) (a) Shi, M.; Nicholas, K. M. Palladium-Catalyzed Carboxylation of Allyl Stannanes. *J. Am. Chem. Soc.* **1997**, *119*, 5057−5058. (b) Takaya, J. Iwasawa, N. Hydrocarboxylation of Allenes with CO_2 Catalyzed by Silyl Pincer-Type Palladium Complex. *J. Am. Chem. Soc.* **2008**, *130*, 15254–15255. (c) Correa, A.; Martín, R. Palladium-Catalyzed Direct Carboxylation of Aryl Bromides with Carbon Dioxide. *J. Am. Chem. Soc.* **2009**, *131*, 15974–15975. (d) Hruszkewycz, D. P.; Wu, J.; Hazari, N.; Incarvito, C. D. Palladium(I)-Bridging Allyl Dimers for the Catalytic Functionalization of CO_2. *J. Am. Chem. Soc*. **2011**, *133*, 3280–3283. (e) Takaya, J.; Sasano, K.; Iwasawa, N. Efficient One-to-One Coupling of Easily Available 1,3-Dienes with Carbon Dioxide. *Org. Lett.* **2011**, *13*, 1698–1701. (f) Mita, T.; Higuchi, Y.; Sato, Y. Highly Regioselective Palladium-Catalyzed Carboxylation of Allylic Alcohols with CO_2. *Chem. Eur. J.* **2015**, *21*, 16391–16394. (g) Zhang, S.; Chen, W.-Q.; Yu, A.; He, L.-N. Palladium-Catalyzed Carboxylation of Benzyl Chlorides with Atmospheric Carbon Dioxide in Combination with Manganese/Magnesium Chloride. *ChemCatChem*, **2015**, *7*, 3972–3977. (h) Higuchi, Y.; Mita, T.; Sato, Y. Palladium-Catalyzed Intramolecular Arylative Carboxylation of Allenes with CO_2 for the Construction of 3-Substituted Indole-2-carboxylic Acids. *Org. Lett*. **2017**, *19*, 2710−2713.

(11) (a) Shen, K.; Han, X.; Lu, X. Cationic Pd(II)-Catalyzed Reductive Cyclization of Alkyne-Tethered Ketones or Aldehydes Using Ethanol as Hydrogen Source. *Org. Lett.* **2013**, *15*, 1732–1735. (b) Shen, K.; Han, X.; Xia, G.; Lu, X. Cationic Pd(II)-Catalyzed Cyclization of N-tosyl-aniline Tethered Alkynyl Ketones Initiated by Hydropalladation of Alkynes: a Facile Way to 1,2-Dihydro or 1,2,3,4-tetrahydroquinoline Derivatives. *Org. Chem. Front*. **2015**, *2*, 145–149.

(12) (a) Wu, W.; Jiang, H. Palladium-Catalyzed Oxidation of Unsaturated Hydrocarbons Using Molecular Oxygen. *Acc. Chem. Res*. **2012**, *45*, 1736-1748. (b) Wu, W.; Jiang, H. Haloalkynes: A Powerful and Versatile Building Block in Organic Synthesis. *Acc. Chem. Res.* **2014**, *47*, 2483−2504. (c) Zhang, Y.; Xiong, W.; Cen, J.; Yan, W.; Wu, Y.; Qi, C.; Wu, W.; Jiang, H. Direct Bromocarboxylation of Arynes using Allyl Bromides and Carbon Dioxide. *Chem. Commun.* **2019**, *55*, 12304-12307. (d) Jiang, H.; Zhang, Y.; Xiong, W.; Cen, J.; Wang, L.; Cheng, R.; Qi, C.; Wu, W. A Three-Phase Four-Component Coupling Reaction: Selective Synthesis of *o*-Chloro Benzoates by KCl, Arynes, CO_2, and Chloroalkanes. *Org. Lett.* **2019**, *21*, 345−349.

(13) (a) Van Leeuwen, P. W. N. M. Homogeneous Catalysis: Understanding the Art; Kluwer Academic Publishers: The Netherlands, **2004**. (b) Williams, D. B. G.; Shaw, M. L.; Hughes, T. *Organometallics* **2011**, *30*, 4968–4973.

(14) More details see the Supporting Information.

(15) CCDC 1974010 (**5c**) contains the supplementary crystallographic data for this paper. These data can be obtained free of charge from The Cambridge Crystallographic Data Centre via www.ccdc.cam.ac.uk/data_reques/cif.

(16) Li, J.; Shen, J.; Xia, C.; Wang, Y.; Liu, D.; Zhang, W. Asymmetric Hydrogenation of *α*-Substituted Acrylic Acids Catalyzed by a Ruthenocenyl Phosphino-oxazoline−Ruthenium Complex. *Org. Lett*. **2016**, *18*, 2122−2125.

(17) Covaleda, G.; Gallego, P.; Vendrell, J.; Georgiadis, D.; Lorenzo, J.; Dive, V.; Aviles, F. X.; Reverter, D.; Devel, L. Synthesis and Structural/Functional Characterization of Selective M14 Metallocarboxypeptidase Inhibitors Based on Phosphinic Pseudopeptide Scaffold: Implications on the Design of Specific Optical Probes. *J. Med. Chem*. **2019**, *62*, 1917−1931.

(18) CCDC 1975009 (**6**) contains the supplementary crystallographic data for this paper. These data can be obtained free of charge from The Cambridge Crystallographic Data Centre via www.ccdc.cam.ac.uk/data_reques/cif.

(19) (a) Zhang, S.; Mei, Q.; Liu, H.; Liu, H.; Zhang, Z.; Han, B. Copper-catalyzed *N*-formylation of Amines with CO_2 under Ambient Conditions. *RSC Adv.* **2016**, *6*, 32370–32373. (b) Huang, Z.; Jiang, X.; Zhou, S.; Yang, P.; Du, C.-X.; Li, Y. Mn - Catalyzed Selective Double and Mono - *N* - Formylation and *N* - Methylation of Amines by using CO_2. *ChemSusChem* **2019**, *12*, 3054–3059.

(20) (a) Wang, Q.; Jia, J.-F.; Guo, C.-H.; Wu, H.-S. Mechanistic Investigationof Cu(I)-mediated Three-component Domino Reaction of Asymmetrical Alkynes with Carbon Dioxide: Theoretical Rationale for the Regioselectivity. *J. Organomet. Chem.* **2013**, *748*, 84−88. (b) Choi, J.-C.; Shiraishi, K.; Takenaka, Y.; Yasuda, H.; Sakakura, T. Synthesis and Reactivity of Five-Membered Palladalactones from Arylallenes and Carbon Dioxide: Relevance to Catalytic Lactone Synthesis. *Organometallics* **2013**, *32*, 3411−3414.

(21) (a) Chai, J. D.; Head-Gordon, M. Long-range Corrected Hybrid Density Functionals with Damped Atom–Atom Dispersion Corrections. *Phys. Chem. Chem. Phys.* **2008**, *10*, 6615−6620. (b) Lee, C.; Yang, W.; Parr, R. G. Development of the Colle-Salvetti Correlation-energy Formula into a Functional of the Electron Density. *Phys. Rev. B.* **1988**, *37*, 785−789. (c) Hay, P. J.; Wadt, W. R.; Kahn, L. R. Ab Initio Effective Core Potentials for Molecular Calculations. II. All-electron Comparisons and Modifications of the Pro-cedure. *J. Chem. Phys*. **1978**, *68*, 3059−3066. (d) Marenich, A. V.; Cramer, C. J.; Truhlar, D. G. Universal Solvation Model Based on Solute Electron Density and on a Continuum Model of the Solvent Defined by the Bulk Dielectric Constant and Atomic Surface Tensions. *J. Phys. Chem. B.* **2009**, *113*,

6378−6396. (e) Marenich, A. V.; Cramer, C. J.; Truhlar, D. G.; Universal Solvation Model Based on Solute Electron Density and on a Continuum Model of the Solvent Defined by the Bulk Dielectric Constant and Atomic Surface Tensions. *J. Phys. Chem. B.* **2009**, *113*. 6378-6396.

(22) (a) Hermans, J.; Wang, L. Inclusion of Loss of Translational and Rotational Freedom in Theoretical Estimates of Free Energies of Binding. Application to a Complex of Benzene and Mutant T4 Lysozyme. *J. Am. Chem. Soc.* **1997**, *119*, 2707−2714. (b) Mammen, M.; Shakhnovich, E. I.; Deutch, J. M.; Whitesides, G. M. Estimating the Entropic Cost of Self-Assembly of Multiparticle Hydrogen-Bonded Aggregates Based on the Cyanuric Acid Melamine Lattice. *J. Org. Chem.* **1998**, *63*, 3821−3830. (c) Sakaki, S.; Takayama, T.; Sumimoto, M.; Sugimoto, M. Theoretical Study of the Cp_2Zr-Catalyzed Hydrosilylation of Ethylene. Reaction Mechanism Including New σ-Bond Activation. *J. Am. Chem. Soc*. **2004**, *126*. 3332−3348. (d) Li, H.; Zhao, L.; Lu, G.; Mo, Y.; Wang, Z.-X. Insight Into the Relative Reactivity of "Frustrated Lewis pairs" and Stable Carbenes in Activating H_2 and CH_4: A Comparative Computational Study. *Phys. Chem. Chem. Phys*. **2010**, *12*, 5268−5275. (e) Li, l.-F.; Zhu, H.-J.; Liu, L.; Song, D.-T.; Lei, M. A Hydride-Shuttle Mechanism for the Catalytic Hydroboration of CO_2. *Inorg. Chem.* **2018**, *57*, 3054−3060.

(23) Cioslowski, J. A New Population Analysis Based on Atomic Polar Tensors. *J. Am. Chem. Soc.* **1989**, *111*, 8333−8336.